JOURNAL OF PROPULSION AND POWER
Vol. 9, No. 6, Nov.-Dec. 1993

Wind-Tunnel Evaluation of Mid-Airframe Installed Turbojet Engines

J. S. Lilley*
U.S. Army Missile Command, Redstone Arsenal, Alabama 35898
and
S. L. Pengelly†
Boeing Defense and Space Group, Huntsville, Alabama 35898

A series of power-on wind-tunnel tests have been conducted to evaluate the installed performance of mid-airframe mounted tactical-missile turbojet sustainers. Two low-cost, expendable turbojet engine designs were installed in a high-fidelity wind-tunnel model of a specific tactical missile. To accommodate the unique installation requirements, each engine design incorporated bifurcated pitot inlets and side-exhausting bifurcated exhaust ducts. Each installed engine was fully functional and was intended to closely replicate the in-flight operational response. Power-on wind-tunnel evaluations were conducted for each engine model that encompassed a wide range of sea level, steady-state flight conditions. The test condition variables evaluated were Mach number, pitch angle, yaw angle, engine throttle setting, and control fin deflection. Missile axial force data were acquired to determine installed, delivered engine net thrust. In addition, extensive thermal instrumentation was installed on the model to evaluate the influence of the turbojet exhaust plume on the aft section of the missile. A detailed description of the test program is provided. Detailed descriptions of the hardware configuration and test variables are presented. Presented are discussions of theoretical engine performance models, experimental installed performance results, projections of overall missile performance, and evaluations of the effect of pitch on engine performance. A detailed evaluation of the thermal impact of turbojet operation is provided. Discussions of the thermal impact of pitch, yaw, and fin deflection angles are presented. The results presented demonstrate that both sustainer configurations, successfully operated in an installed configuration under in-flight conditions, delivered adequate installed performance to satisfy missile system requirements, and had minimal adverse thermal impact on the airframe. The results of the evaluation fully verify the viability of employing turbojet engines in a mid-airframe installation.

Nomenclature

A_{jet} = jet nozzle area, in.^{2}
F = net thrust, corrected, lbf
F_{ax} = missile axial force, corrected, lbf
I_p = optimization index of performance, lbf^2
M = Mach number
N = engine speed, corrected, krpm
P = pressure, psia
R = range per fuel weight, km/lbm
S/N = engine serial number
SFC = specific fuel consumption, corrected, lbm/h-lbf
T = temperature, °F
V = flight speed
$\dot{W}_f$ = fuel flow rate, lbm/h
α = pitch angle, deg
β = yaw angle, deg
Δ = difference
δ = pressure correction factor
θ = temperature correction factor

Subscripts
a = ambient
max = maximum possible
min = minimum possible or measured
mes = measured
off = power-off
on = power-on
pred = cycle deck prediction
T_{max} = maximum temperature
T_{min} = minimum temperature
$t2$ = inlet total

Presented as Paper 92-3752 at the AIAA/SAE/ASME/ASEE 28th Joint Propulsion Conference and Exhibit, Nashville, TN, July 6–8, 1992; received Aug. 31, 1992; revision received March 20, 1993; accepted for publication April 13, 1993.

*Aerospace Engineer, Propulsion Directorate. Senior Member AIAA.
†Mechanical Engineer.

Introduction

FOR a number of tactical missile applications, an expendable turbojet engine is an attractive alternative for the sustainer propulsion system. A turbojet sustainer offers the inherent advantages of on-demand thrust variability, high fuel efficiency, minimum visible and infrared signatures, and compliance with insensitive munitions requirements. In a traditional tactical missile installation, the turbojet sustainer engine is mounted at the extreme aft end of the airframe with a rear exiting axial exhaust. However, the design requirements of several future missile systems necessitate the location of guidance and control equipment (i.e., wire reels, fiber optic bobbins, laser receivers) in the rear of the missile, forcing the turbojet sustainer to be installed in the midsection of the airframe. To accommodate mid-airframe operations, a convenient design approach is to integrate the turbojet engine with a bifurcated pitot inlet system and a bifurcated side-exiting exhaust system. Operation of a turbojet engine in such a configuration, however, raises significant design and performance concerns for the entire missile system. To successfully develop a missile utilizing a mid-airframe installed turbojet sustainer, the following technical concerns must be adequately addressed:

1) Will the turbojet engine, configured in a mid-airframe installation, successfully operate under all required flight conditions?

2) Will the turbojet sustainer deliver adequate installed performance to satisfy missile system requirements?

3) Will the side-exiting exhaust system have an adverse thermal impact on the aft section of the missile airframe?

In order to comprehensively address the above issues, an extensive experimental test program was undertaken, which involved the testing of a full-scale aerodynamic model of a turbojet-powered tactical missile in a transonic wind tunnel. Presented in the following sections is a detailed description of the evaluation that was conducted.

Hardware Configuration

The wind-tunnel model used in the test program was a high-fidelity, full-scale, representation of a turbojet powered tactical missile. The pertinent features of the model are shown in Fig. 1. The model incorporates four wings and four control fins, each of which has a rectangular planform. The wings are mounted directly to the turbojet sustainer section which is in the midsection of the airframe. Inlets and exhausts are located in line with each other, and each of two inlet-exhaust pairs are positioned circumferentially between a pair of wings. The mouth of each inlet is positioned ahead of the leading edge of the wings, and the exit plane of the exhausts is aft of the wing trailing edge. The fins are in line with the wings, and consequently, each exhaust is nominally oriented between a pair of fins. The missile was designed to fly with the wings in a cruciform, "X," configuration with inlets and exhausts located on either side of the airframe (Fig. 1 depicts the airframe as being rolled 90 deg from nominal with the inlets on top and bottom). The missile was designed for "skid-to-turn," and the inlets were intended to be maintained in a level, horizontal attitude during turning maneuvers.

Presented in Fig. 2 is a cross section of the model that provides a number of critical airframe dimensions (in inches) and illustrates the overall planform geometry. Note that the missile station numbers of critical geometric features are also included. The airframe body is essentially cylindrical (7.0-in. o.d.), with a hemispherical nose. The airframe bulges to a maximum of 8.0 in. in diameter in the sustainer section to accommodate the turbojet engine and attachment of the wings. Other significant airframe features (which are evident in Fig. 1) are a wiring race cover that runs nearly the length of the entire airframe, and simulated actuator covers located under each fin. From Figs. 1 and 2, it is evident that the presence of inlets, exhausts, and the wire race results in a very asymmetric configuration.

The model was designed for the installation and operation of two different turbojet engine designs. Unique sustainer sections were developed for both the WJ119 turbojet engine and for the Model TJ-90. Both turbojet engines are nominally 7.0-in.-diam, 100-lbf thrust class, (static, sea-level uninstalled, standard day), single-spool turbojet engines. Each sustainer had unique inlet and exhaust designs. Descriptions of the WJ119 and TJ-90 are given in Ref. 1. Illustrations of both engines are presented in Fig. 3.

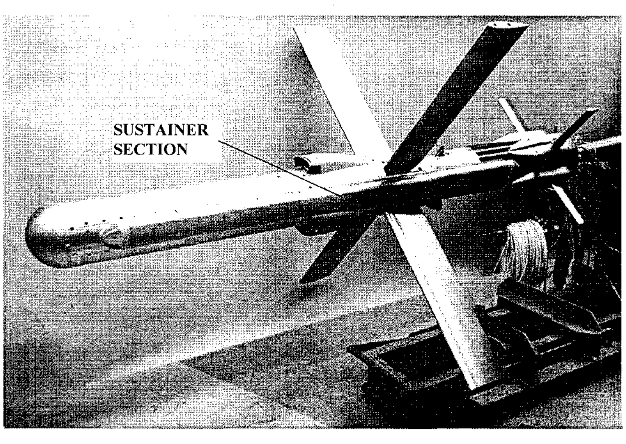

Fig. 1 Power-on wind-tunnel model.

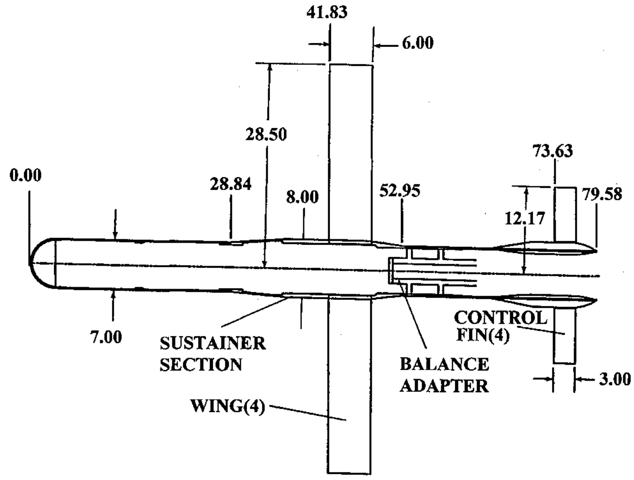

Fig. 2 Power-on wind-tunnel model cross section.

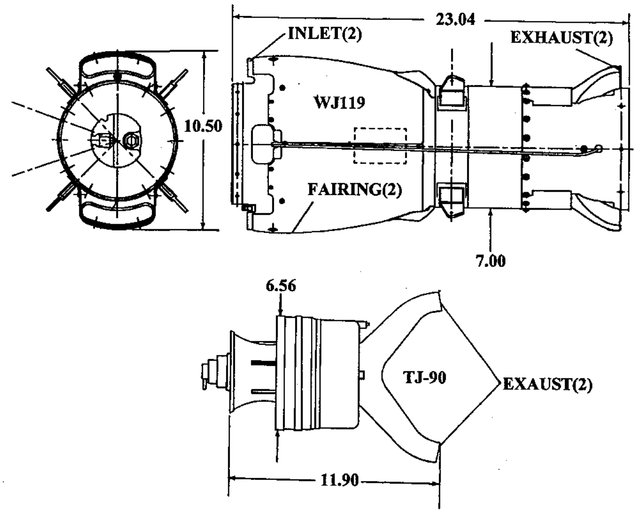

Fig. 3 Turbojet sustainer engines.

The wind-tunnel model was installed on an axial sting mount system (shown in Fig. 1) in the test section of the wind tunnel. The test facility used during this test program was an 8-ft transonic wind tunnel. During test operations the sting assembly (with the model) could be remotely pitched through a range of angles (positive and negative) without reconfiguring the model. To evaluate yaw angles, the model was rolled 90 deg (as in Fig. 1) and the remote pitch facility employed. To evaluate the impact of control fin deflections, each fin was manually configurable over a range of angles.

To obtain data to sufficiently characterize the performance of the tactical missile represented by the model, three distinct sets of instrumentation were used: 1) aerodynamic, 2) thermal, and 3) engine. The aerodynamic instrumentation consisted primarily of a six-component balance that was used to measure all forces and moments transmitted to the airframe (the location of the balance is shown in Fig. 2). In addition, a multicomponent (three or six) balance was installed on each fin to obtain control authority data. The thermal instrumentation was intended to measure the impact of the engine exhaust plume on the aft section of the airframe. Numerous thermocouples and heat-flux gauges were mounted on the airframe body and on the fins to provide detailed thermal data. The engine instrumentation was provided to allow engine health monitoring and to provide engine performance data. Thermocouples and pressure taps were installed in the inlets, throughout the engine, and in the exhaust. Engine rotational speed and fuel flow rate data were also acquired. A total of 72 channels of instrumentation were installed on the model. To achieve and maintain successful sustainer operation, a personal computer-based control system (which was located remotely outside the wind tunnel) was responsible for the execution of all phases of sustainer operation. A detailed description of the personal computer based system is presented in Ref. 1.

Variables/Measurements

Presented in Table 1 is a summary of the independent test variables that were selected for evaluation, along with the range over which each was evaluated. The range of independent variables was selected to reflect the anticipated operating conditions of the missile system. The tactical missile under consideration was intended to be used as a ground launched system that operated at a relatively low flight altitude. Accordingly, operating altitude was not considered a test variable, and all tests were conducted at simulated sea level ambient pressures. The test facility was a closed circuit wind tunnel with no capability for air temperature control. Consequently, air temperature was not a test variable, and the available tunnel ambient temperature T_a was used in all tests. For convenience, all applicable test results were corrected to sea level, standard day, ambient conditions.

The dependent test measurements generated for each power-on test can be characterized in three basic groups: 1) engine performance, 2) missile performance, and 3) thermal (missile aft surface temperatures).

For the purposes of this evaluation, only two engine performance parameters are relevant: 1) corrected (to standard conditions) engine rotational speed N, and 2) corrected fuel flow rate $\dot{W}_f$. These values are determined by the following relationships:

$$N = N_{\text{mes}}/\sqrt{\theta} \tag{1}$$

$$\dot{W}_f = \dot{W}_{f\text{mes}}/(\delta\sqrt{\theta}) \tag{2}$$

The subscript mes denotes an uncorrected measurement

$$\theta = T_{t2}/518.67°\text{R} \tag{3}$$

$$\delta = P_a/14.696 \text{ psia} \tag{4}$$

where T_{t2} is the measured inlet total temperature, and P_a is the wind-tunnel ambient pressure.

The relevant missile performance parameters are corrected F, SFC, and corrected R. These parameters are determined by the following relationships:

$$F = F_{\text{ax on}} - F_{\text{ax off}} \tag{5}$$

where $F_{\text{ax on}}$ is the corrected power-on axial force, and $F_{\text{ax off}}$ is the corrected power-off axial force.

The value of $F_{\text{ax on}}$ is the corrected net force measured along the missile axis when the engine is operating, and $F_{\text{ax off}}$ is the associated measurement made when the engine was not operating. To obtain values of $F_{\text{ax off}}$, for every power-on run made with an operating engine, a corresponding run was made with an installed, but nonoperating engine. During power-off runs, air was allowed to flow through the inlets and the engine freely windmilled. The assumption made in Eq. (5) was that the difference between the power-on and power-off corrected axial force measurements (for a given configuration and set of flight conditions) was the corrected net installed thrust. The drag contribution of the unpowered, wind-milling engine was neglected from the force accounting procedure [Eq. (5)]. As a consequence, the net thrust values that were calculated were reduced slightly by this unaccounted drag (therefore introducing a level of conservatism). Given the limitations of the instrumentation, test hardware, and facilities available, the thrust accounting procedure utilized was the most accurate means of determining engine thrust. The following relationships were used to correct the axial force measurements:

$$F_{\text{ax on}} = F_{\text{ax on mes}}\delta \tag{6}$$

$$F_{\text{ax off}} = F_{\text{ax off mes}}\delta \tag{7}$$

The values of SFC and R are given by the following relationships:

$$\text{SFC} = \dot{W}_f/F \tag{8}$$

$$R = V/\dot{W}_f \tag{9}$$

where V is the standard day flight velocity:

$$V = M(1224.81 \text{ km/h}) \tag{10}$$

The thermal measurements consisted primarily of the data acquired from the previously discussed instrumentation channels. Additional thermal data consisted of an average engine exhaust gas temperature (EGT), obtained through the engine data acquisition system. It should be noted that all thermal measurements were reported as actual data and were not corrected to standard conditions.

After the selection of the relevant independent test variables and dependent performance measurements, a test matrix was established for the power-on test program. The type of evaluations conducted can be characterized as follows.

1) Engine/Missile Performance Evaluations

The airframe was held level ($\alpha = 0$ deg), straight ($\beta = 0$ deg), with zero fin deflection, at a fixed Mach number, and the engine speed was varied. These tests were conducted for a range of Mach numbers.

2) Engine/Missile Pitch Evaluation

Engine speed and Mach number were held constant, and airframe was swept through a range of pitch angles. The yaw and fin deflection angle were held at zero. These tests were conducted for various combinations of engine speed and Mach number.

3) Missile Yaw Evaluation

Engine speed and Mach number were held constant, and the airframe was swept through a range of yaw angles. The pitch and fin deflection angles were held at zero. These tests were conducted for various engine speeds and Mach numbers.

4) Thermal Fin Deflection

Engine speed and Mach number were held constant, and the fin deflection angle on all four fins was set to a nonzero value. For each test the airframe was swept through a range of pitch angles while holding the yaw angle at zero. These tests were conducted for various combinations of engine speed, Mach number, and fin deflection angle. Note that the first three test types were performed with both engine models. Fin deflection evaluations were not considered for the TJ-90.

Table 1 Independent power-on test variables

Test variable	Range evaluated
M	0.05, 0.10, 0.33, 0.40, 0.50, 0.55, 0.60, 0.65
α, deg	−16–16
β, deg	−12–12
N, WJ119, krpm	41–55
N, TJ-90, krpm	59–99
Fin deflection, deg	−16, −12, −8, 0

While data from all 72 channels was acquired during all test types, for the purposes of this evaluation, not all data were relevant or even accurate. For test type 1, performance data (engine and missile) was of primary interest, and consequently, the thermal data was not evaluated. For test type 2, both performance and thermal data were of interest and evaluated. For test types 3 and 4, the large number of cables and engine services crossing the balance rendered all axial force data (power-on and power-off) inaccurate. Consequently, for these tests, only thermal data was evaluated. It can be recalled that for each power-on test (for all types), a corresponding power-off run was conducted. Those power-off results were only employed for test types 1 and 2.

For each engine model, two individual engines (designated by serial number) were used, both of which were intended to be similar in performance and representative of the engine type. As the test results will show, this was not always the case. It must be noted that individual power-off tests were conducted for both the WJ119 (*S/N* 301 and 302) model configurations. Consequently, installed performance values will reflect the specific power-off data for each WJ119 engine. Only a single set of power-off data was generated for the TJ-90 configurations (utilizing both *S/N* 18 and 23).

Theoretical Engine Models

Theoretical performance prediction codes (cycle decks) were obtained from the manufacturers for each engine. The respective cycle decks each accounted for installation effects by the incorporation of models for both the bifurcated pitot inlets (based on wind-tunnel data) and the bifurcated exhausts. It should be noted that pitch and yaw influences on sustainer performance were not accounted for. For each engine model, two versions of the cycle deck were provided: 1) a specification version (SPEC) which represented a sustainer that delivered the minimum acceptable performance, and 2) a status version (STAT) which represented the performance of a nominal production engine.

An initial step in validating the cycle decks was the calibration of the models to match the performance of each individual engine (designated by serial number). For each engine (*S/N*), the data from acceptance test procedures (ATP), model check-out tests, and low Mach number (less than or equal to 0.10) wind-tunnel tests were used to calibrate the respective cycle decks. For both the appropriate SPEC and STAT cycle decks, each corrected calibration data set (N, M, F) was used as input, and an optimization search was performed on the exhaust area, A_{jet}, to minimize the following index of performance I_p:

$$I_p = \sum (F_{pred} - F_{mes})^2 \qquad (11)$$

For each engine (*S/N*) the cycle deck type (SPEC or STAT), when utilizing the optimum A_{jet}, which produced the lowest I_p, represented the calibrated cycle deck for that engine.

Presented in Table 2 are the results of the cycle deck calibrations. For each engine, the particular cycle deck selected (SPEC or STAT) and the optimum exhaust areas are provided. For reference purposes, exhaust areas for the SPEC and STAT decks for each engine model are included. Also presented in Table 2 are installed performance predictions for static, sea level, standard day operation at idle and maximum power settings. Predictions are presented for all four engines that were tested and for each standard SPEC and STAT deck.

Also presented in Table 2 are the minimum M_{min}, and maximum M_{max}, possible installed flight Mach number for each engine. These Mach numbers are based on sea level, standard day, straight and level operation in the tactical missile airframe evaluated in this investigation, and correspond to the idle and maximum engine power settings. For all four TJ-90 engine models, a single drag model (based on power-off tests with the installed sustainer) was used to determine the Mach numbers. For the WJ119 models, the *S/N* 301 drag model was used for that engine and the *S/N* 302 drag model was used in the other three cases.

From the results in Table 2, it can be seen that the performance model for *S/N* 23 closely matches that of a status engine. However, the performance model for *S/N* 18 is best represented by a STAT deck with a significantly reduced exhaust area. This result indicates that during either acceptance testing or model installation, the exhaust area of *S/N* 18 was incorrectly sized. As a consequence, *S/N* 18 has a significantly different cycle match (as compared to *S/N* 23) and experienced elevated exhaust gas temperatures at high throttle settings. It should be noted that the maximum engine speed for *S/N* 18 was limited by turbine inlet temperature (or EGT), not by mechanical speed (as was the case for all other engines). For *S/N* 301 and 302, the performance model for both engines closely matches the SPEC deck. Consequently, both engines can be expected to exhibit the minimum (specification) level of performance.

From the results in Table 2, it can also be seen that both TJ-90 engines are capable of propelling the missile airframe at Mach numbers between 0.26–0.57. For the WJ119 engines, the range is 0.32–0.54. It must be noted that even though *S/N* 301 and 302 have virtually identical performance models, the Mach number range for each is different. This discrepancy is a result of differences in the drag models used for each engine. Overall, on the basis of the theoretical models (and drag data), each engine design has sufficient thrust to operate the airframe over an adequate Mach number range. However, these results require experimental verification.

Installed Engine Performance

Presented in Figs. 4 and 5 are some of the results of the power-on installed performance evaluations for both engine models. Presented are plots of net installed corrected thrust and net installed corrected fuel consumption given as a function of corrected engine speed. Data are presented for a given engine *S/N* operating at a fixed Mach number, with zero pitch, yaw, and fin deflection angles. Data was acquired from both engine/missile performance evaluations (type 1 tests) and engine/missile pitch evaluations (type 2 tests) at pitch equal zero points. Both individual data points (denoted by the descrete symbols) and theoretical predictions (denoted by smooth curves) are provided for each data set.

The results presented in Figs. 4 and 5 indicate that over the range of Mach numbers evaluated, both engines demonstrated the following: 1) successful operation over the full range of engine throttle settings (idle to maximum); 2) the delivery of significant net thrust to the missile airframe at the maximum throttle setting; 3) fuel efficient operation over the entire throttle range, but in particular at maximum power; and 4) the ability to deliver a continuum of net thrust levels to the airframe through on-demand throttle control.

These results clearly demonstrate the successful operation of both engine designs as a mid-airframe, mounted tactical missile turbojet sustainer. The successful operation and high performance (thrust and specific fuel consumptions) of each sustainer verify the effectiveness of the respective bifurcated pitot inlet and bifurcated side-exiting exhaust systems (however, sufficient instrumentation was not available to fully characterize inlet and exhaust efficiencies).

From the results presented in Figs. 4 and 5, some general observations can be made concerning the installed performance of each engine model. The results in Figs. 4 and 5 permit a direct performance comparison of the two WJ119 engines. From these results, it can be seen that *S/N* 302 consistently had higher thrust and lower SFC than *S/N* 301. However, static test data used to calibrate the cycle decks indicated that both engines had virtually identical performance and essentially were SPEC engines. As was previously discussed,

Table 2 Theoretical performance summary

			Static, sea level, standard day, installed								Installed flight vehicle, performance limits	
			Idle				Maximum					
	Engine/deck	A_{jet}, in.^{2}	N, krpm	F, lbf	SFC, lbm/h-lbf	EGT, °F	N, krpm	F, lbf	SFC, lbm/h-lbf	EGT, °F	M_{min}	M_{max}
TJ-90	18/STAT	4.456	60	20.49	2.0861	920	98.5	97.74	1.3828	1672	0.26	0.57
	23/STAT	4.931	60	18.68	2.1524	860	102	95.77	1.3180	1503	0.25	0.57
	SPEC	5.050	60	13.94	2.9314	1034	102	96.71	1.4439	1656	0.22	0.57
	STAT	4.900	60	18.79	2.1476	863	102	96.84	1.3219	1521	0.25	0.57
WJ119	301/SPEC	5.689	42	35.6	1.905	1139	55.847	88.6	1.450	1519	0.32	0.54
	302/SPEC	5.697	42	35.5	1.906	1138	55.847	88.3	1.450	1515	0.28	0.55
	SPEC	5.700	42	35.5	1.907	1137	55.847	88.2	1.449	1513	0.28	0.55
	STAT	5.700	42	35.3	1.614	1071	55.847	95.1	1.304	1443	0.28	0.57

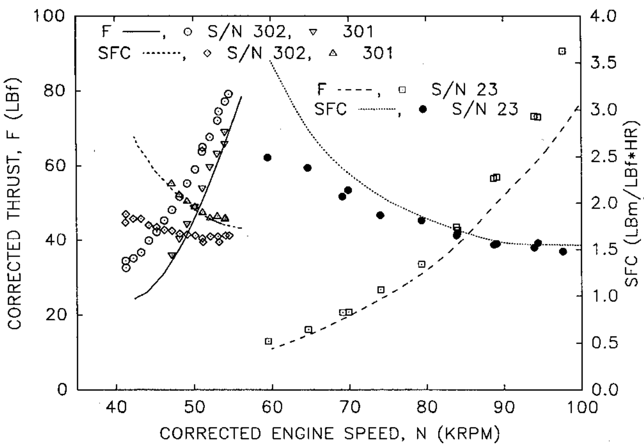

Fig. 4 Installed performance (M = 0.33).

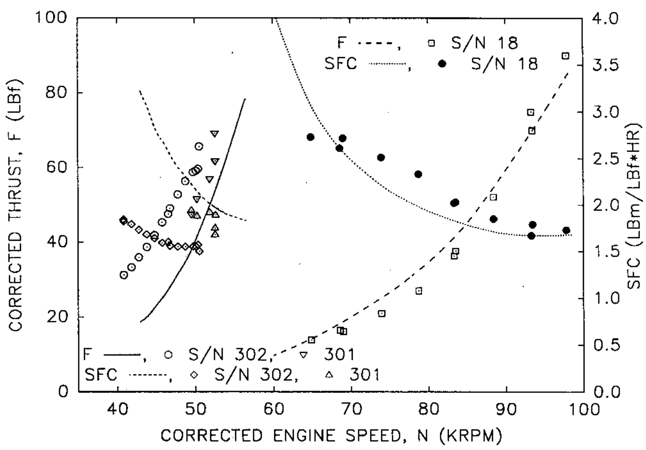

Fig. 5 Installed performance (M = 0.50).

separate power-off axial force data sets were used to determine the installed thrust [using Eq. (5)] for each engine. The performance differences between the two engines can most likely be attributed to the application of the individual drag models in the force accounting data reduction procedures. The power-off data used for *S/N* 302 indicated higher drag levels than that employed for *S/N* 301. If, in actuality, the airframe drag and engine performance were equivalent for both engines during power-on testing, then the use of the higher drag levels in the reduction of the performance data for *S/N* 302 would provide an explanation for the observed thrust increase and SFC decrease for that engine (relative to *S/N* 301). The justification for utilizing individual drag data sets for each WJ119 engine was that power-on and power-off data were acquired for a given model build and calibration series. Consequently, any force measurement biases associated with the particular build would tend to be cancelled out during the application of Eq. (5). The question to be answered is which power-off data set is the most representative of the airframe drag. The answer to that question is beyond the scope of this engine performance investigation. Accordingly, the drag models were used "as is," and the validation of those models was left to a subsequent investigation, the results of which are presented in Ref. 2.

An additional observation is that for all Mach numbers, at the maximum power setting, the TJ-90 engines exhibited markedly higher thrust than the WJ119 engines. This result is a consequence of the fact that the TJ-90 engines both approached STAT performance (even though *S/N* 18 was trimmed differently), while the WJ119 engines closely matched SPEC performance. This performance difference is clearly illustrated in Table 2. From Table 2, it can also be seen that STAT WJ119 and TJ90 engines would have virtually equivalent performance.

The installed performance data presented in Figs. 4 and 5 were used to validate the calibrated cycle decks for each engine. With regard to the WJ119, in Fig. 4, there is excellent agreement between the experimental results and the performance predictions for *S/N* 301, for both thrust and SFC. In Fig. 5 there is once again good agreement between experimental results and predictions for *S/N* 301. In both Figs. 4 and 5 there is a distinct off-set between experimental results and predictions for *S/N* 302, which is most probably a consequence of the drag model used and not inaccuracies in the cycle deck. However, despite these discrepancies, the experimental results for *S/N* 302 matched the predicted performance trends.

For the case of the TJ90, the predictions in Fig. 4 indicate very good agreement with the experimental results (both thrust and SFC) for *S/N* 23. Similarly, good agreement is exhibited in Fig. 5 for *S/N* 18. This good agreement for *S/N* 18 validates the representation of that engine as a STAT TJ-90 with a significantly reduced exhaust area.

Overall, the results presented in Figs. 4 and 5 serve to validate the cycle decks by demonstrating the ability to predict, in-flight, installed net performance (thrust and SFC), over a full range of throttle settings for various Mach numbers. Given the inherent inaccuracies in the experimental power-on and power-off force measurements (due to the large number of items crossing the balance), the level of agreement achieved between predictions and data was more than suitable for validation purposes. The test program results verify that SPEC and STAT cycle decks for each respective engine are valid representations of installed turbojet sustainer performance and are suitable for incorporation in an overall missile simulation.

Missile Performance

Installed performance data and the calibrated (and validated) cycle decks were used to evaluate in-flight performance of the tactical missile airframe when operating with each of the sustainer engines. Curve-fits of installed performance and power-off drag data were used to determine engine operating points (throttle settings) at which F_{axon} was zero (thrust-equals-drag). Corresponding theoretical thrust-equals-drag engine operating curves were also generated using the cycle decks for each engine (SPEC, STAT, and individual engines). For the case of the WJ119 engines, the corresponding drag models were employed for each individual engine and the drag model of *S/N* 302 was used for the SPEC and STAT analyses (as it was the most conservative). The results of these engine operating point evaluations are presented in Figs. 6 and 7. Presented in Fig. 6 are the thrust-equals-drag engine speeds plotted as a function of Mach number. Presented in Fig. 7 are the corresponding R values [as determined by Eq. (9)] plotted as a function of Mach number.

The most significant observation that can be made from Fig. 6 is that sustained cruise at Mach numbers between 0.33 and 0.50 was experimentally demonstrated with either engine installed in the missile. While the respective cycle decks predict an even greater Mach number range (refer to Table 2), the data points in Fig. 6 represent experimentally measured thrust-equals-drag operation and conclusively demonstrated the ability of each turbojet to function as a tactical missile sustainer.

The most significant observation that can be made from Fig. 7 is that over the Mach number range evaluated, both sustainer designs experimentally demonstrated excellent fuel efficiency. For the case of the TJ-90, missile range per fuel weight values R in excess of 8.0 km/lbm were demonstrated at Mach 0.33, and R values in excess of 5.5 km/lbm at Mach 0.50. For the WJ119, R values in excess of 6.4 km/lbm were demonstrated at Mach 0.33, and R values in excess of 5.3 km/lbm at Mach 0.50. If the assumption is made that a cylindrical fuel tank is used with an i.d. of 6.5 in. (for installation in the 7.0-in. o.d. airframe), and the fuel used is JP-10 (as was the case in all the experimental evaluations), then 1.114 lbm of fuel can be accommodated per inch of fuel tank length. Operation at a R value of 5.3 km/lbm translates into 5.9 km per inch of fuel tank length. Thus, the results presented in Fig. 7 experimentally demonstrate that the tactical missile design that was considered can achieve significant ranges (in excess of 5.9 km/in.), at acceptable flight Mach numbers (in excess of 0.50), while being sustained by either of the turbojet engine designs.

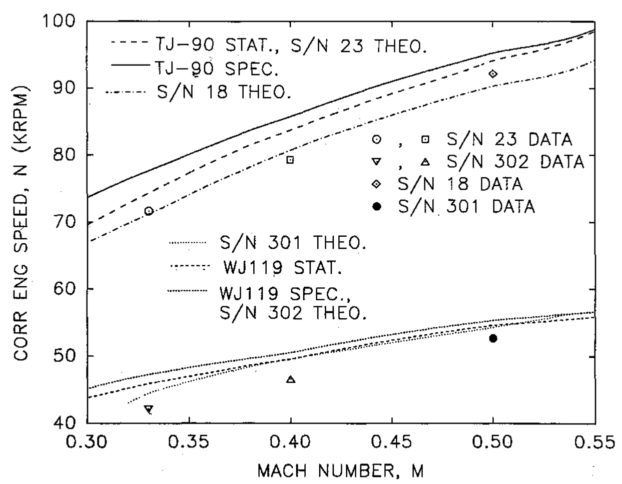

Fig. 6 Required engine speeds for flight vehicle cruise conditions.

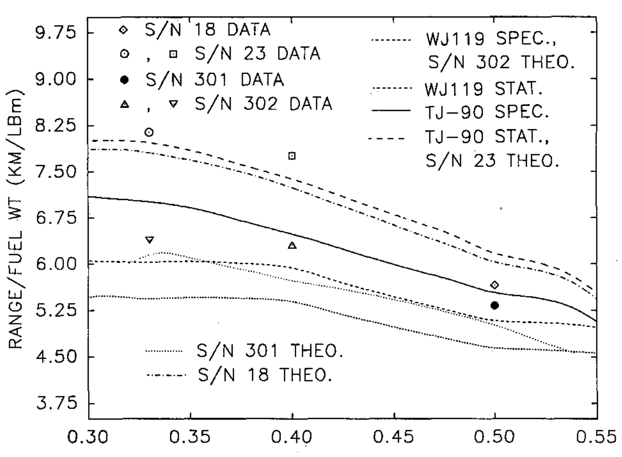

Fig. 7 Range per fuel weight for flight vehicle cruise conditions.

Pitch Influences on Performance

The previously discussed experimental evaluations were concerned with installed sustainer performance during straight and level flight. Additional evaluations (type 2 tests) were conducted to determine the impact of pitch maneuvers on installed sustainer performance. Presented in Fig. 8 is a plot of installed corrected thrust as a function of pitch angle for TJ-90, *S/N* 23, for Mach 0.33, at various engine speeds. The results in Fig. 8 are typical for both engines at Mach 0.33 and 0.50. For both engine models, for all cases evaluated, there was no degradation in thrust (as compared to the zero pitch condition) for ranges of pitch angles in excess of ± 10 deg. These results indicate that the inlet system for both sustainer functioned acceptably over the demonstrated pitch range. The pitch range that was demonstrated more than adequately encompasses the anticipated operating range of the missile system. Consequently, the results illustrated in Fig. 8 demonstrate successful operation and nondegraded installed performance during pitch maneuvers. It should be noted that successful yaw operation was demonstrated, but performance results were not evaluated due to previously discussed reasons. The results of the pitch evaluations also justify the use of the cycle decks for installed performance predictions, despite the fact that pitch influences were neglected in the respective inlet models.

Thermal Evaluation

Data from the wind-tunnel evaluation (test types 2–4) were also used to determine the thermal effects caused by a hot engine exhaust impinging on the aft missile body and fins. This thermal data was acquired to evaluate maximum surface temperatures in these areas and to understand what factors affected the aft missile environment. This evaluation was intended to satisfy the third technical concern.

Thermal data collection, which ran concurrently with performance data collection, was done at various angles of α, β,

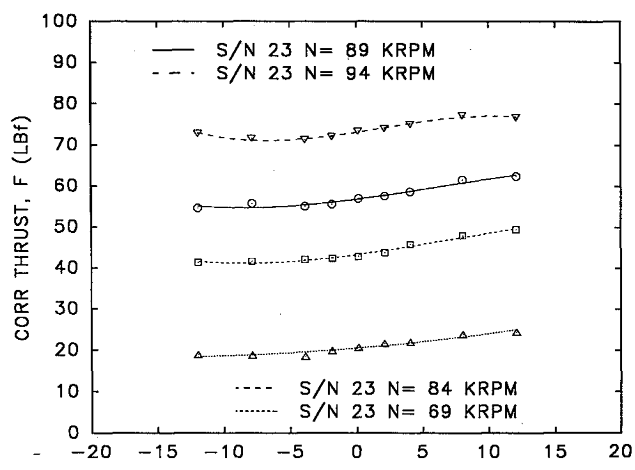

Fig. 8 Typical influence of pitch on installed thrust (TJ-90, M = 0.33).

and fin deflections. Data for α and β variations were considered at two different Mach numbers ($M = 0.33$ and 0.50) and with both engine models to determine temperature effects along the missile body and fins. Thermal data evaluating fin deflection effects were collected with only the WJ119 engine installed. A description of the instrumentation and a discussion of the data follows.

Thermal Instrumentation and Its Arrangement

Thermal data were acquired using standard beaded-end type-K thermocouples. These thermocouples were installed from the inside of the missile airframe and extended through the airframe into the free airstream a distance of approximately $\frac{1}{2}$ in. To allow measurement of temperature gradients along the missile body, thermocouples were placed at different fuselage stations as shown in Fig. 9. The total number of thermocouples used for evaluating thermal data was 12, and their placement was such that temperature gradients along the missile could be measured in both the horizontal and vertical planes. The horizontal plane was defined as running through the engine axis and both exhaust nozzles. The vertical plane was defined as running through the engine axis but perpendicular to the exhaust nozzles. There were eight thermocouples in the horizontal plane and four in the vertical. The thermocouples in the first three stations of the horizontal plane were paired on the left and right sides of the missile body. The remaining two unpaired thermocouples in the horizontal plane were used to measure temperatures leading into the area of the fin actuator covers. In like manner, the thermocouples in the vertical plane were paired on the upper and lower missile body and fins. Note that the two thermocouples at station 74.05, on the fins, reside in a vertical plane horizontally displaced from the forward two vertical thermocouples at station 64.02.

Discussion of Thermal Data

The results of thermal evaluations are summarized in Tables 3–6. Additional detailed data (in graphical form) from the thermal evaluation are presented in Ref. 3. The thermal data are separated into three categories: 1) the effects of pitch (Tables 3 and 4), 2) the effects of yaw (Table 5), and 3) the effects of fin deflections (Table 6). All three categories of data were examined at $M = 0.33$ and 0.50, and except for fin deflection effects, all categories of data came from wind-tunnel tests using both the WJ119 and the TJ-90 turbojet engines. Fin deflection effects data were acquired only with the WJ119 engine. In all categories, data were taken when the engines were at or near full power and the corresponding average exhaust gas temperatures (average EGT) are given.

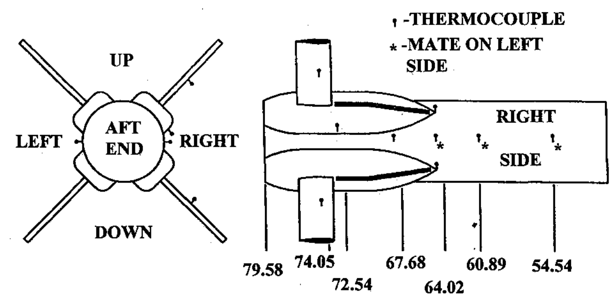

Fig. 9 Thermocouple installation.

Trends in Maximum Temperature as a Function of Pitch

In general, temperatures as a function of pitch along the aft missile body and fins varied between 150–400°F (Tables 3 and 4). Minimum temperatures were slightly above or near ambient (75–100°F). The maximum change in temperature ΔT_{max} at any one station was between 135–200°F. Missile aft body temperatures were generally the highest (approximately 400°F) and the lowest (approximately 150°F) were on the fins. These results were generally expected as the exhaust nozzles were directed along the aft body. The fins, being away from the aft body, straddling the exhaust plume, and immersed in the freestream, would be subject to less heating. However, an unexpected result is that throughout all degrees of pitch, the WJ119 engine consistently heated the aft body and fins more (approximately 75–100°F) than did the TJ-90 engine—even though average EGT between the two models was nearly equal. These results indicate that the design of the TJ-90 exhaust system was superior to that of the WJ119 from the standpoint of thermal impact on the missile.

The effect of Mach number on temperature for pitch maneuvers was not as evident as the engine model influences. For example, the left side maximum temperatures with the WJ119 at $M = 0.33$ and at $M = 0.50$ were 400°F; whereas the right side maximum temperatures were 350°F at $M = 0.33$ and 225°F at $M = 0.50$. Adding to this asymmetrical temperature trend was the fact that the maximum temperatures occurred at diverse pitch angles: $\alpha_{T_{max}}$ at $M = 0.33$ was -7 or -16 deg as opposed to 11 deg at $M = 0.50$. Mach effects with the TJ-90 engine were also peculiar: maximum temperatures on the left side decreased from 325 to 300°F with a change from $M = 0.33$ to 0.50, while the right side increased from 250 to 330°F. In addition, $\alpha_{T_{max}}$ changed from +8 deg (both sides) at $M = 0.33$ to -8 deg (left side) and +8 deg (right side). There is no viable explanation for the temperature trends with respect to Mach number and pitch.

Mach effects on temperature vs pitch in the vertical plane were more consistent. As Mach number increased, temperatures on the fins decreased. For example, on the upper fins with the WJ119 operating at $M = 0.33$, $T_{max} = 250$°F and at $M = 0.50$, $T_{max} = 150$°F. The drop in temperature apparently was due to the cooling effect of the higher speed wind-tunnel air.

Trends in Maximum Temperature as a Function of Yaw

The thermal effects of yaw in the horizontal plane can be seen in Table 5. No trends due to yaw were noted in the vertical plane, accordingly, no data for the vertical plane are presented. As can be seen in Table 5, T_{max} for the missile in yaw was 400°F on the right side with the TJ-90 engine operating at both Mach 0.33 and 0.50. Simultaneously, the left side of the missile varied from 200°F at $M = 0.33$ to 280°F at $M = 0.50$. With the WJ119 operating, maximum temperatures were slightly lower (50–100°F), but the sides where

Table 3 Thermal effects of α in the horizontal plane

Mach no.	Engine model	T_{max}, °F	Station$_{T_{max}}$, in.	$\alpha_{T_{max}}$, deg	ΔT_{max}, °F	T_{min}, °F	Station$_{T_{min}}$, in.	Average EGT, °F	α Range, deg
0.33	WJ119	400(LS) 350(RS)	64.02	−7(LS) −16(RS)	200	100	72.54	1433	±16
0.33	TJ90	325(LS) 250(RS)	60.89(LS) 64.02(RS)	8	175	80	67.68 and 72.54	1430	±16
0.50	WJ119	400(LS) 225(RS)	54.54	11	135	140	67.68 and 72.54	1310	−4 to 11
0.50	TJ90	300(LS) 330(RS)	60.89 54.54	8 −8	160	75	72.54	1366	±8

Table 4 Thermal effects of α in the vertical plane

Mach no.	Engine model	T_{max}, °F	Station$_{T_{max}}$, in.	$\alpha_{T_{max}}$, deg	ΔT_{max}, °F	T_{min}, °F	Station$_{T_{min}}$, in.	Average EGT, °F	α Range, deg
0.33	WJ119	250(UF) 300(LF)	Fins (74.05)	+16 −16	200	100	64.02 and Fins	1433	±16
0.33	TJ90	190(UF) 225(LF)	Fins (74.05)	+16 −16	135	90	64.02 and Fins	1430	±16
0.50	WJ119	150(LF)	Fins (74.05)	11	60	90	64.02 and Fins	1310	−4 to 11
0.50	TJ90	N/A	N/A	N/A	Nil	90	64.02 and Fins	1366	±8

Table 5 Thermal effects of β in the horizontal plane

Mach no.	Engine model	T_{max}, °F	Station$_{T_{max}}$, in.	$\beta_{T_{max}}$, deg	ΔT_{max}, °F	T_{min}, °F	Station$_{T_{min}}$, in.	Average EGT, °F	β Range, deg
0.33	WJ119	350(LS) 290(RS)	60.89(LS) 64.02(RS)	−12(LS) −12(RS)	40	150	67.68	1473	−12 to 4
0.33	TJ90	200(LS) 400(RS)	60.89(LS) 54.54(RS)	8	75	150	67.68	1402	−12 to 8
0.50	WJ119	300(LS) 190(RS)	54.54(LS) 64.02(RS)	2	40	130	67.68	1278	−4 to 2
0.50	TJ90	280(LS) 400(RS)	60.89 60.89	7	75	150	67.68	1441	−4 to 7

Table 6 Thermal effects of α on the fins

Mach no.	Engine model	Fin deflection, deg	T_{max}, °F	$\alpha_{T_{max}}$, deg	ΔT_{max}, °F	T_{min}, °F	Average EGT, °F	α Range, deg
0.33	WJ119	−8	220(UF) 75(LF)	+16	145	75	1402	−4 to 16
0.33	WJ119	−12	225(UF) 300(LF)	−16 +16	225	75	1480	±16
0.33	WJ119	−16	280(UF) 280(LF)	+16 −18	205	75	1334	−18 to 16
0.50	WJ119	−8	150(UF) 75(LF)	+12	75	150	1402	−4 to 12
0.50	WJ119	−12	150(UF) 75(LF)	+12	75	75	1209	±16
0.50	WJ119	−16	75(UF) 170(LF)	−10	95	75	1230	−10 to 5

the maximum temperatures occurred were opposite to those of the TJ-90. For instance, on the left side of the missile with the WJ119 engine operating at $M = 0.33$, T_{max} was 350°F, while the 400°F T_{max} mentioned above occurred on the right side. This reversal of sides where T_{max} occurred at $M = 0.50$ as well and indicates a different hot-gas plume flowfield distribution, from one side to the other dependent on which engine is operating.

Another significant observation is that the maximum change in temperature ΔT_{max} at any station was only 40–75°F, whereas during pitch changes ΔT_{max} was much higher, 135–200°F. This difference in ΔT_{max} between pitch and yaw makes sense since the hot exhaust bathes both sides of the fuselage throughout all degrees of yaw; whereas in pitch the relative wind would deflect the exhaust away from the missile body during even small pitch angles.

Trends in Maximum Temperature as a Function of Fin Deflection

Table 6 presents data regarding the thermal effects of fin deflection while the WJ119 was operating. Note in the data of Table 6, the lower fin thermocouple evidently was not working as it indicated the ambient temperature. Consequently, for this discussion only the upper fin data will be considered. This data was generated by repeating the pitch evaluations using various fin deflections (type 4 tests). Consequently, comparisons between the data in Table 4 (thermal effects of pitch in the vertical plane) and Table 6 (thermal effects of pitch in the vertical plane at various fin deflections) should indicate the influence of fin deflection.

Note in Table 6 that the greatest T_{max} was 300°F (fin deflection = −16 deg, $M = 0.33$); in Table 4 it was 300°F (fin deflection = −16 deg, $M = 0.33$) as well. In both sets of data, T_{max} occurred at high pitch (±16 deg, approximately). At fin deflections other than −16 deg, the fin temperature was less, but not significantly. Note further that the trend of lowered T_{max} at higher Mach number seen in Table 4 was repeated in Table 6. At $M = 0.33$, T_{max} (upper fin) = 250°F with no fin deflection and T_{max} (upper fin, all fin deflections) = 220–280°F; and at $M = 0.50$ T_{max} (upper fin) = 150°F with no fin deflection; and following the trend, T_{max} (upper fin, all fin deflections) = 75–150°F. Thus, the results suggest that there was no significant thermal effect due to fin deflections.

Summary of Thermal Effects

Maximum temperatures seen in all configurations discussed above was approximately 400°F. Minimums were at or near ambient temperatures. Maximum range in temperature at any one station was about 200°F. Most often, though not always, the hottest spots were those nearest the exhausts. The most significant factor to contribute to high temperatures was extreme pitch and this seemed to affect mostly the horizontal plane thermocouples. Yaw effects were not as severe as pitch effects. Fins did see high temperatures, as much as 280°F, but only at extreme pitch. Extreme pitch and extreme fin deflections did not seem to worsen fin temperatures any more than extreme pitch alone.

The evaluation results indicate that for both engine models there is no adverse thermal impact on the airframe under flight conditions during level flight or during pitch and yaw maneuvers. In addition, for a full range of fin deflections, there was no severe interaction between the plume and the control surfaces (fins). Overall, the results of the evaluation indicate that a mid-airframe mounted turbojet sustainer, from the thermal impact standpoint, is a fully viable concept. Consequently, the thermal evaluation fully satisfies technical concern 3 (addressed in the Introduction section of this article).

Conclusions

A comprehensive wind-tunnel evaluation of the installed performance of mid-airframe mounted tactical missile turbojet sustainers has been performed. Two unique turbojet sustainer designs were each installed in a tactical missile airframe model, and power-on evaluations were conducted with each engine for a wide range of flight Mach numbers, engine throttle settings, vehicle attitudes, and control surface deflections. Both sustainer configurations demonstrated successful operation over a wide range of Mach numbers (0.1–0.6), pitch angles (±16 deg), yaw angles (±12 deg), and throttle settings (idle to maximum). Both sustainer configurations demonstrated sufficient installed thrust to sustain the tactical missile airframe over a continuum (due to the demonstrated throttling capability) of flight Mach number from 0.33 to 0.50. Each sustainer design demonstrated excellent fuel efficiency providing R values that exceeded 6.4 km/lbm at Mach 0.33 and exceeded 5.3 km/lbm at Mach 0.50. The thermal impact of the sustainer plume for both engine models was evaluated for both pitch and yaw maneuvers at Mach 0.33 and 0.50. In addition, a thermal evaluation of the WJ119 plume was conducted for pitch maneuvers, using a range of fin deflection angles (−16, −12, and −8 deg) for both Mach numbers. The results of the thermal evaluations indicated that for all cases that were considered, plume re-attachment did not occur, there was no significant missile aft section heating, and there was minimal interaction between the plume and the control fins. In addition, with the exception of extreme maneuver angles, the results indicate minimal interaction between the plume and the control fins.

The results of the evaluation program conclusively address the initial technical concerns regarding a mid-airframe-mounted turbojet sustainer by demonstrating that 1) both sustainers operate successfully in an installed configuration under the required flight conditions; 2) both sustainers deliver adequate installed performance (thrust and range) to satisfy missile system requirements; and 3) the side-exit exhaust systems of both sustainers have no adverse thermal impact on the aft airframe.

Consequently, the results of the program demonstrate that a mid-airframe turbojet installation is a viable concept for a tactical missile sustainer propulsion system. In addition, two unique turbojet sustainer designs have experimentally demonstrated performance and operability, are modeled with validated cycle decks, and are available for immediate tactical missile system application.

Acknowledgments

The authors would like to express their appreciation to John Michael Bush of Uwohali, Inc.; to Randall David Huckaby and Lamar Auman of the U.S. Army Missile Command, to Michael Bak and Leo Wasageshik of Williams International, to Anthony Jones and Eugene Miller of Sundstrand Power Systems, to Charles Reed and numerous others at CALSPAN Corp. (Buffalo, New York, wind tunnel), to Royal Harrison, Tom Andrews, and numerous others at the Jet Propulsion Laboratory, for the support provided during all phases of this experimental evaluation.

References

[1]Lilley, J. S., Pengelly, S. L., and Fisher, P., "The PC as a Generic Fuel Control for Expendable Turbojet Engines," AIAA Paper 91-3399, June 1991; see also *Journal of Propulsion and Power*, Vol. 8, No. 6, 1992, pp. 1258–1265.

[2]Auman, L. M., "Wind Tunnel Investigation of a Missile with an Operational Mid-Body Turbojet Engine," AIAA Paper 93-0036, Jan. 1993.

[3]Lilley, J. S., and Pengelly, S. L., "Wind Tunnel Evaluation of the Installed Performance of Mid-Airframe Mounted Tactical Missile Turbojet Sustainers," AIAA Paper 92-3752, July 1992.